*J. Astrophys. Astr.* (2016) 37: 16
DOI: 10.1007/s12036-016-9392-y

# Photometric Analysis and Period Investigation of the EW Type Eclipsing Binary V441 Lac

K. Li[1,2,*], S.-M. Hu[1], D.-F. Guo[1], Y.-G. Jiang[2], D.-Y. Gao[1] & X. Chen[1]
[1]*Shandong Provincial Key Laboratory of Optical Astronomy and Solar-Terrestrial Environment, Institute of Space Sciences, Shandong University, Weihai 264209, China.*
[2]*Key Laboratory for the Structure and Evolution of Celestial Objects, Chinese Academy of Sciences, Kunming, China.*
[*]*e-mail: likai@ynao.ac.cn*

Received 21 January 2016; accepted 29 April 2016

**Abstract.** Four color light curves of the EW type eclipsing binary V441 Lac were presented and analyzed by the W–D code.It is found that V441 Lac is an extremely low mass ratio ($q = 0.093 \pm 0.001$) semi-detached binary with the less massive secondary component filling the inner Roche lobe. Two dark spots on the primary component were introduced to explain the asymmetric light curves. By analyzing all times of light minimum, we determined that the orbital period of V441 Lac is continuously increasing at a rate of $dP/dt = 5.874(\pm 0.007) \times 10^{-7}$ d yr$^{-1}$. The semi-detached Algol type configuration of V441 Lac is possibly formed by a contact configuration destroyed shallow contact binary due to mass transfer from the less massive component to the more massive one predicted by the thermal relaxation oscillation theory.

*Key words.* Stars: binaries: close—stars: binaries: eclipsing—stars: individual: V441 Lac.

## 1. Introduction

Eclipsing binaries are ideal testbeds for a number of astrophysical studies. Based on high-quality radial velocity curves and photometric light curves of eclipsing binaries, one can determine fundamental mass and radius measurements for both components. According to the shape of the light curves, eclipsing binaries can be divided into three types: EA, EB and EW. EW type eclipsing binaries show continuous light variation, and the difference between the depths of the two minima is very small. Although such binaries have been analyzed a lot, a satisfactory theory for their origin, structures and evolution is not complete. More observations and studies for such systems are needed.

 

V441 Lac was first identified to be an eclipsing binary by Agerer (2001) when he started a photometric study of IU Lac. Agerer concluded that the light variability of V441 Lac shows an EW type and the orbital period is $0^d.308894$. After that, a lot of eclipsing times were determined by many investigators (e.g., Agerer & Hubscher 2002, 2003; Hubscher 2011). Recently, Wang *et al.* (2015) analyzed multiple color light curves and the orbital period changes of V441 Lac. They found that V441 Lac is a semi-detached binary with the less massive component filling the inner Roche lobe and that the orbital period of V441 Lac is secular increasing at a rate of $5.67\times10^{-7}$ d/yr. In this paper, we present the $BVR_cI_c$ light curves and the orbital period variation of V441 Lac.

## 2. Observations

CCD photometric observations of V441 Lac were carried out on August 28 and September 4, 2014 using the 1.0-m Cassegrain telescope at Weihai Observatory of Shandong University. The Andor DZ936 camera attached to the telescope was used during the observations. The effective field-of-view is about $12' \times 12'$. The information of the 1.0-m Cassegrain telescope can be identified in Hu *et al.* (2014). The standard Johnson–Cousins–Bessel $BVR_cI_c$ filters were used and the corresponding exposure times for each filter are 80, 60, 40 and 30 s, respectively. During the observations, the readout noise is 7, the gain is 2, and the readout time is about 2 s. The observed data were processed using the IMRED and APPHOT packages in IRAF[1] procedure, including bias and flat-field correction, and aperture photometry. The information of the comparison and check stars is listed in Table 1. The determined light curves with photometric errors in the four bands are shown in the upper panel of Fig. 1, and the differences between the comparison and the check stars are displayed in the lower panel of Fig. 1. The standard deviations of the differences between the comparison and the check stars are 0.0067 in $B$ band, 0.0036 in $V$ band, 0.0047 in $R_c$ band, and 0.0042 in $I_c$ band, respectively. The phases were calculated using the following equation:

$$\text{Min. I} = \text{HJD2456905.08114} + 0.^d30891501E. \quad (1)$$

Two new times of light minimum were determined to be 2456898.13018±0.00028 and 2456905.08114±0.00049.

## 3. Orbital period variation

The period variation of V441 Lac was first studied by Wang *et al.* (2015). As in Wang *et al.* (2015), the $O-C$ times were firstly calculated by the linear ephemeris published by Agerer (2001). Using the least squares method, they determined a new linear ephemeris and constructed a new $O-C$ diagram. A long term period increase at a rate of $5.67\times10^{-7}$ d/yr was derived by them. By combining the times of light

[1] IRAF is distributed by the National Optical Astronomy Observatories, which is operated by the Association of Universities for Research in Astronomy Inc., under contract to the National Science Foundation.

**Table 1.** Informations of V441 Lac, the comparison, and the check stars.

| Stars | Name | $\alpha_{2000}$ | $\delta_{2000}$ | mag ($B$) | mag ($R$) | References |
|---|---|---|---|---|---|---|
| Variable | V441 Lac | $22^h09^m37^s.53$ | $+52°34'16''.0$ | 12.6 | 12.2 | Morrison *et al* (2001) Samus *et al.* (2003) |
| Comparison | GSC 03969-02134 | $22^h09^m47^s.36$ | $+52°35'55''.0$ | 12.8 | 11.8 | Zacharias *et al.* (2004) |
| Check | GSC 03969-02680 | $22^h09^m42^s.12$ | $+52°32'33''.0$ | 13.6 | 12.3 | Zacharias *et al.* (2004) |

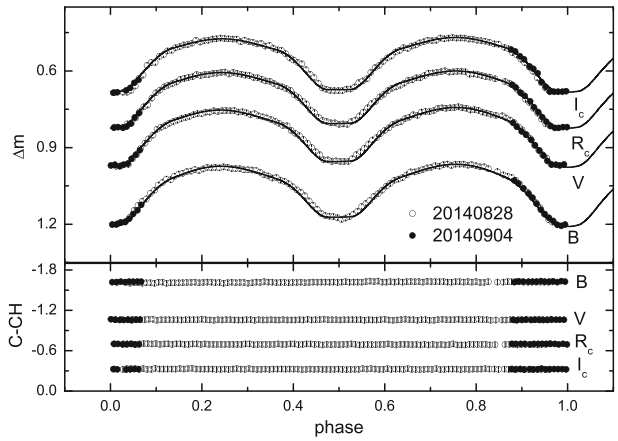


**Figure 1.** The $BVR_cI_c$ light curves of V441 Lac. The open circles represent the data determined on August 28, while the solid ones display the data determined on September 4. The photometric errors are also shown in this figure. The error bars are not clear because they are less than the size of the symbols.

minimum in the literature and our two new determined ones, we analyzed the $O-C$ behavior of V441 Lac. The same linear ephemeris taken from Wang *et al.* (2015) was used to calculated the $O-C$ values. All eclipsing times and the $O-C$ values are listed in Table 2, and the corresponding $O-C$ diagram is displayed in the upper panel of Fig. 2.

As seen in Fig. 2, the $O-C$ values show an upward parabolic trend. Using the least squares method, we determined the following quadratic ephemeris:

$$\text{Min. I} = \text{HJD}2451817.5488(2) + 0^d.308911589(5)E + 2.484(3) \times 10^{-10}E^2. \quad (2)$$

Based on the quadratic term of this ephemeris, a secular orbital period increase rate of $\mathrm{d}P/\mathrm{d}t = 5.874(\pm 0.007) \times 10^{-7}$ d yr$^{-1}$ was obtained. The residuals from the full ephemeris are displayed in the lower panel of Fig. 2, where no regularity can be found.

## 4. Light curve solutions

The light curve of V441 Lac has been analyzed by Wang *et al.* (2015). They determined that V441 Lac is a semi-detached binary with the less massive secondary

**Table 2.** Times of minimum light for V441 Lac.

| HJD2400000+ | Errors | Method | Type | $E$ | $O-C$ | Residuals | References |
|---|---|---|---|---|---|---|---|
| 51421.8340 | | ccd | p | −1281 | 0.0100 | 0.0005 | Paschke & Brat (2006) |
| 51771.3699 | | ccd | s | −149.5 | 0.0086 | 0.0034 | IBVS 5024 |
| 51771.5226 | | ccd | p | −149 | 0.0068 | 0.0016 | IBVS 5024 |
| 51816.3140 | | ccd | p | −4 | 0.0056 | 0.0008 | IBVS 5024 |
| 51816.4691 | | ccd | s | −3.5 | 0.0062 | 0.0015 | IBVS 5024 |
| 51816.6221 | | ccd | p | −3 | 0.0048 | 0.0000 | IBVS 5024 |
| 51817.5489 | | ccd | p | 0 | 0.0048 | 0.0001 | IBVS 5024 |
| 51838.5548 | | ccd | p | 68 | 0.0045 | 0.0000 | IBVS 5024 |
| 51839.3283 | | ccd | s | 70.5 | 0.0057 | 0.0012 | IBVS 5024 |
| 51839.4831 | | ccd | p | 71 | 0.0060 | 0.0016 | IBVS 5024 |
| 51890.2890 | | ccd | s | 235.5 | −0.0046 | −0.0085 | IBVS 5024 |
| 51901.2644 | 0.0004 | pe | p | 271 | 0.0043 | 0.0005 | IBVS 5296 |
| 52083.5210 | 0.0008 | pe | p | 861 | 0.0011 | −0.0009 | IBVS 5296 |
| 52084.4474 | 0.0004 | pe | p | 864 | 0.0007 | −0.0012 | IBVS 5296 |
| 52113.4867 | 0.0010 | pe | p | 958 | 0.0020 | 0.0004 | IBVS 5296 |
| 52134.4929 | 0.0018 | pe | p | 1026 | 0.0020 | 0.0005 | IBVS 5296 |
| 52194.4180 | 0.0005 | pe | p | 1220 | −0.0024 | −0.0033 | IBVS 5296 |
| 52194.5744 | 0.0056 | pe | s | 1220.5 | −0.0005 | −0.0014 | IBVS 5296 |
| 52228.4033 | 0.0014 | pe | p | 1330 | 0.0022 | 0.0016 | IBVS 5296 |
| 52228.5577 | 0.0005 | pe | s | 1330.5 | 0.0022 | 0.0016 | IBVS 5296 |
| 52505.4952 | 0.0020 | pe | p | 2227 | −0.0026 | −0.0010 | IBVS 5484 |
| 52617.3218 | 0.0038 | pe | p | 2589 | −0.0033 | −0.0008 | IBVS 5484 |
| 52621.3363 | 0.0023 | pe | p | 2602 | −0.0047 | −0.0022 | IBVS 5484 |
| 52875.4197 | 0.0024 | pe | s | 3424.5 | −0.0039 | 0.0002 | IBVS 5657 |
| 53222.4834 | 0.0005 | pe | p | 4548 | −0.0062 | −0.0005 | IBVS 5657 |
| 53226.5004 | 0.0031 | pe | p | 4561 | −0.0051 | 0.0007 | IBVS 5657 |
| 53242.4039 | 0.0007 | pe | s | 4612.5 | −0.0107 | −0.0049 | IBVS 5657 |
| 53255.3831 | 0.0063 | pe | s | 4654.5 | −0.0059 | −0.0001 | IBVS 5657 |
| 53255.5357 | | pe | p | 4655 | −0.0078 | −0.0019 | IBVS 5657 |
| 53256.4653 | 0.0006 | pe | p | 4658 | −0.0049 | 0.0009 | IBVS 5657 |
| 53258.4723 | 0.0004 | pe | s | 4664.5 | −0.0059 | 0.0000 | IBVS 5657 |
| 53259.4008 | 0.0013 | pe | s | 4667.5 | −0.0041 | 0.0017 | IBVS 5657 |
| 53259.5528 | 0.0002 | pe | p | 4668 | −0.0066 | −0.0007 | IBVS 5657 |
| 53614.5041 | 0.0015 | pe | p | 5817 | 0.0014 | 0.0082 | IBVS 5731 |
| 53653.4210 | 0.0032 | pe | p | 5943 | −0.0050 | 0.0018 | IBVS 5731 |
| 53932.5262 | 0.0016 | pe | s | 6846.5 | −0.0045 | 0.0025 | IBVS 5731 |
| 54031.3758 | 0.0017 | pe | s | 7166.5 | −0.0077 | −0.0007 | IBVS 5761 |
| 54718.4054 | 0.0005 | pe | s | 9390.5 | −0.0051 | 0.0004 | IBVS 5984 |
| 54718.5595 | 0.0005 | pe | p | 9391 | −0.0055 | 0.0001 | IBVS 5984 |
| 55058.5237 | 0.0012 | pe | s | 10491.5 | −0.0022 | 0.0016 | IBVS 5941 |
| 55062.3821 | 0.0011 | pe | p | 10504 | −0.0053 | −0.0015 | IBVS 5941 |
| 55062.5379 | 0.0010 | pe | s | 10504.5 | −0.0039 | −0.0001 | IBVS 5941 |
| 55309.5174 | 0.0046 | pe | p | 11304 | −0.0020 | 0.0003 | IBVS 5959 |
| 55463.3571 | 0.0008 | pe | p | 11802 | −0.0020 | −0.0009 | IBVS 5984 |
| 55463.5131 | 0.0035 | pe | s | 11802.5 | −0.0004 | 0.0007 | IBVS 5984 |
| 55477.7211 | 0.0010 | ccd | s | 11848.5 | −0.0025 | −0.0015 | IBVS 5960 |
| 55806.4070 | 0.0027 | pe | s | 12912.5 | −0.0022 | −0.0041 | IBVS 6026 |
| 55806.5648 | 0.0021 | pe | p | 12913 | 0.0012 | −0.0008 | IBVS 6026 |
| 55808.4186 | 0.0021 | pe | p | 12919 | 0.0015 | −0.0005 | IBVS 6026 |
| 55839.3121 | 0.0020 | pe | p | 13019 | 0.0035 | 0.0012 | IBVS 6026 |
| 55839.4642 | 0.0039 | pe | s | 13019.5 | 0.0011 | −0.0011 | IBVS 6026 |
| 55873.2928 | 0.0021 | pe | p | 13129 | 0.0035 | 0.0009 | IBVS 6026 |
| 56187.4619 | 0.0013 | pe | p | 14146 | 0.0061 | 0.0001 | IBVS 6070 |
| 56187.6135 | 0.0042 | pe | s | 14146.5 | 0.0032 | −0.0028 | IBVS 6070 |

**Table 2.** (*Continued*).

| HJD2400000+ | Errors | Method | Type | $E$ | $O-C$ | Residuals | References |
|---|---|---|---|---|---|---|---|
| 56570.0583 | 0.0004 | ccd | s | 15384.5 | 0.0112 | 0.0004 | Wang *et al.* (2015) |
| 56570.2120 | 0.0002 | ccd | p | 15385 | 0.0104 | −0.0004 | Wang *et al.* (2015) |
| 56574.0737 | 0.0001 | ccd | s | 15397.5 | 0.0107 | −0.0002 | Wang *et al.* (2015) |
| 56590.2932 | 0.0017 | pe | p | 15450 | 0.0122 | 0.0011 | IBVS 6118 |
| 56590.4460 | 0.0017 | pe | s | 15450.5 | 0.0105 | −0.0006 | IBVS 6118 |
| 56592.3027 | 0.0025 | pe | s | 15456.5 | 0.0138 | 0.0026 | IBVS 6118 |
| 56592.4559 | 0.0015 | pe | p | 15457 | 0.0125 | 0.0013 | IBVS 6118 |
| 56600.3327 | 0.0013 | pe | s | 15482.5 | 0.0120 | 0.0007 | IBVS 6118 |
| 56600.4870 | 0.0017 | pe | p | 15483 | 0.0118 | 0.0005 | IBVS 6118 |
| 56898.1302 | 0.0003 | ccd | s | 16446.5 | 0.0154 | −0.0003 | This paper |
| 56905.0811 | 0.0005 | ccd | p | 16469 | 0.0157 | 0.0000 | This paper |
| 56934.2735 | 0.0009 | pe | s | 16563.5 | 0.0156 | −0.0006 | IBVS 6152 |
| 56934.4287 | 0.0030 | pe | p | 16564 | 0.0164 | 0.0002 | IBVS 6152 |
| 56934.5833 | 0.0022 | pe | s | 16564.5 | 0.0165 | 0.0003 | IBVS 6152 |

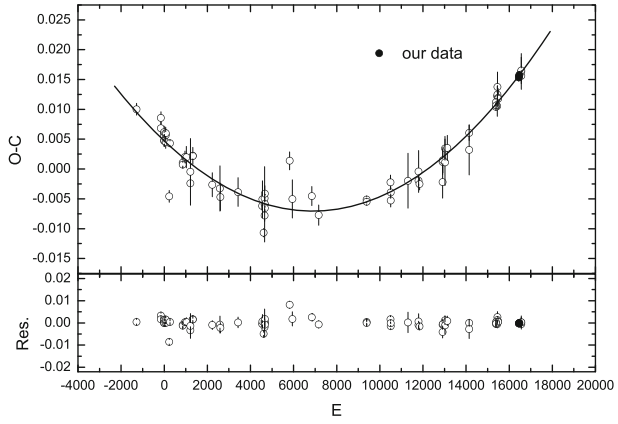


**Figure 2.** The $O-C$ diagram of V441 Lac. The open circles represent the eclipsing times from literatures, while the solid ones display the eclipsing times given by us. The minima that have no errors were set as 0.0010.

component filling the inner Roche lobe and has a mass ratio of $q = 0.15$. We used the Wilson–Devinney (W–D) code (Wilson & Devinney 1971; Wilson 1990, 1994) to investigate our new derived four light curves simultaneously. W–D code is based on the Roche model and is a tool for the modeling of eclipsing binaries by real photometric and radial velocity data. Different sets of photometric data of the same object gives different parameters. The spots on the solution can affect the values of the parameters. Many investigations of binaries have confirmed this, such as the studies of GSC 03526-01995 (Liao *et al.* 2012), EP And (Lee *et al.* 2013), and EQ Tau (Li *et al.* 2014).

The effective temperature of primary component was fixed at $T_1 = 7906$ K, which is taken from Wang *et al.* (2015). According to von Zeipel (1924), the gravity-darkening coefficient and the bolometric albedo of the two components were set to be 1.0 for radiative atmospheres ($T_{\rm eff} > 7200$ K). The logarithmic limb darkening law was adopted and limb darkening coefficients were taken from Van Hamme (1993)

according to the filter and temperatures of the components. These parameters were kept constant during all solutions. We adjusted orbital inclination $i$, temperature of the secondary component $T_2$, the dimensionless potentials $\Omega_{1,2}$ and luminosity $L_1$ of the primary component during the solutions.

Since no spectroscopic mass ratio has been obtained for V441 Lac, a $q$-search method was used to determine the mass ratio, meaning that we calculated a series of models with assumed values of mass ratio $q$. During the solutions, the W–D code was started with mode 2 (detached configuration). We found that the solutions can be converged at both mode 4 (the more massive component filling its inner Roche lobe) and mode 5 (the less massive component filling its inner Roche lobe). The weighted sum of the squared residuals, $\sum W_i(O-C)_i^2$, for mode 4 and mode 5 are displayed in Fig. 3. Solid circles represent mode 4, while open ones show mode 5. The minimum value of $\sum W_i(O-C)_i^2$ is found at $q = 0.10$ of mode 5, meaning that solutions with mode 5 can achieve the best fit to the observations. According to the orbital period study, the orbital period of V441 Lac is continuously increasing, revealing a mass transfer from the less massive component to the more massive one. Mode 5 with the less massive component filling its inner Roche lobe is consistent with the result that was gained by the orbital period investigation. Solutions with mode 5 were performed by setting $q = 0.10$ as the initial value and an adjustable parameter. The derived photometric elements are listed in Table 3. As shown in Fig. 1, the two light maxima of V441 Lac have different light levels, indicating that the spot mode of the W–D program should be used in as many other active eclipsing binaries, AD Cnc (Qian *et al.* 2007), PY Vir (Zhu *et al.* 2013) and EQ Tau (Li *et al.* 2014). Iterative testing shows that two dark spots on the primary components with a mass ratio of $q = 0.093 \pm 0.001$ leads to the best fit. The corresponding solution results are listed in Table 3 and the spots parameters are shown in Table 4. The value of $\sum W_i(O-C)_i^2$ for the solution with spots is much smaller than that without spot. Therefore, the solution with two spots is chosen as the final result. The corresponding synthetic light curves are displayed in Fig. 1 and the geometric structure is plotted in Fig. 4.

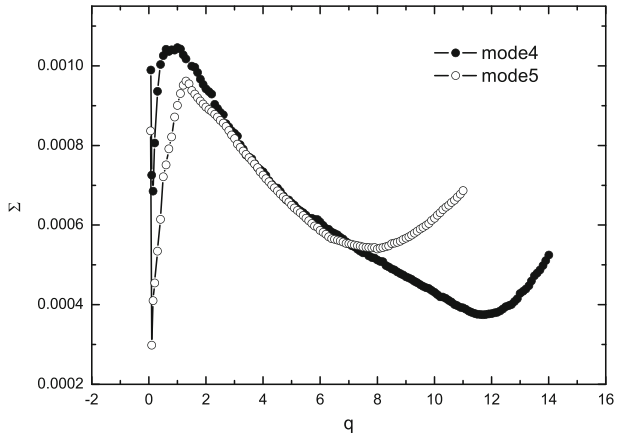


**Figure 3.** $\sum -q$ relation of V441 Lac. Solid circles represent mode 4, while open ones show mode 5.

**Table 3.** Photometric solutions for V441 Lac determined by analyzing the four color light curves simultaneously.

| Parameters | Photometric elements with spots | Errors | Photometric elements without spots | Errors |
|---|---|---|---|---|
| $T_1$ (K) | 7906 | Fixed | 7906 | Fixed |
| $q(M_2/M_1)$ | 0.093 | ±0.001 | 0.090 | ±0.001 |
| $T_2$ (K) | 7290 | ±15 | 7311 | ±18 |
| $i^\circ$ | 73.4 | ±0.2 | 73.4 | ±0.4 |
| $\Omega_1$ | 2.0577 | ±0.0041 | 2.0569 | ±0.0045 |
| $\Omega_2$ | 1.9364 | Fixed | 1.9279 | Fixed |
| $L_{1B}/L_B$ | 0.9145 | ±0.0001 | 0.9145 | ±0.0001 |
| $L_{1V}/L_V$ | 0.9077 | ±0.0001 | 0.9078 | ±0.0001 |
| $L_{1R_c}/L_{R_c}$ | 0.9024 | ±0.0001 | 0.9028 | ±0.0001 |
| $L_{1I_c}/L_{I_c}$ | 0.8976 | ±0.0001 | 0.8983 | ±0.0001 |
| $r_1$(pole) | 0.5063 | ±0.0011 | 0.5059 | ±0.0012 |
| $r_1$(point) | 0.5893 | ±0.0025 | 0.5869 | ±0.0027 |
| $r_1$(side) | 0.5526 | ±0.0015 | 0.5519 | ±0.0017 |
| $r_1$(back) | 0.5643 | ±0.0017 | 0.5632 | ±0.0019 |
| $r_2$(pole) | 0.1856 | ±0.0005 | 0.1840 | ±0.0005 |
| $r_2$(point) | 0.2765 | ±0.0117 | 0.2742 | ±0.0122 |
| $r_2$(side) | 0.1929 | ±0.0005 | 0.1912 | ±0.0005 |
| $r_2$(back) | 0.2237 | ±0.0005 | 0.2219 | ±0.0006 |
| $\Sigma W(O-C)^2$ | 0.00020 | | 0.00026 | |

**Table 4.** Spot parameters for V441 Lac.

| Parameters | $\theta$ (radian) | $\phi$ (radian) | $r$ (radian) | $T_f(T_d/T_0)$ |
|---|---|---|---|---|
| Spot 1 | 1.57 | 3.14 | 0.13 | 0.72 |
| Spot 2 | 2.09 | 4.47 | 0.12 | 0.82 |

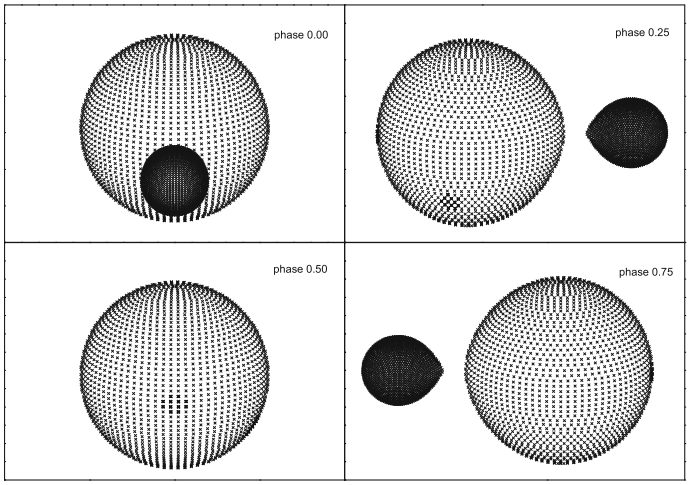


**Figure 4.** The geometric structure of V441 Lac.

## 5. Results and conclusion

The newly observed $BVR_cI_c$ light curves of the EW type eclipsing binary V441 Lac were presented. The four color light curves were simultaneously analyzed by the W–D program. The solution shows that V441 Lac is an extremely low mass ratio ($q = 0.093$) semi-detached binary with the less massive secondary component filling the inner Roche lobe. The primary component fills 94% of its inner Roche lobe. The asymmetric light curves are explained by two dark spots on the primary components. Our results are very different from that determined by Wang *et al.* (2015), such as the mass ratio, the orbital inclination and the effective temperature of the secondary component. The values of Max. I–Max. II, Min. I–Min. II, Min. I–Max. I, and Min. II–Max. II of V441 Lac are listed in Table 5. As shown in this table, the level of Max. I and Max. II is almost the same as in Wang *et al.* (2015). No spot was needed to fit their light curves. However, the values of Max. I–Max. II in B and V bands of our light curves are larger than 0.01. Spot modes should be used to fit our asymmetric light curves. The differences between Min. I and Min. II of Wang *et al.* (2015) is larger than that of our light curves, leading to the difference in the effective temperatures between the two components determined by Wang *et al.* (2015) which is bigger than that derived by us. In addition, the changes of the values of Max. I–Max. II, Min. I–Min. II, Min. I–Max. I and Min. II–Max. II indicate that V441 Lac shows strong magnetic activity.

The reasons that caused the difference of photometric elements between that of Wang *et al.* (2015) and ours are as follows: (1) the shape of the light curve is changed a lot, the depths of the primary minimum and the secondary minimum are different, and the light curves obtained by Wang *et al.* (2015) are almost symmetric whereas ours are asymmetric; (2) V441 Lac is a partially eclipsing binary, making the mass ratio determined only by the photometric light curves less confident (Terrell & Wilson 2005). We suggest that our results are more reliable. Firstly, our results are determined by four color light curves with higher precision,secondly, the orbital inclination derived by us is larger which reveals more reliable photometric elements due to the result of Terrell & Wilson (2005).

The mass of the primary component can be estimated to be $1.84M_\odot$ based on the spectral type of A7 (determined by the effective temperature $T_1 = 7906$ K, Cox 2000) assuming that the primary component is a normal main sequence star. The mass of the secondary can be determined to be $0.17M_\odot$ according to the mass ratio $q = M_2/M_1 = 0.093$. The other physical parameters of V441 Lac can be

**Table 5.** The magnitude differences of V441 Lac.

| Band | Max. I–Max. II | Min. I–Min. II | Min. I–Max. I | Min. II–Max. II | References |
|---|---|---|---|---|---|
| White | −0.018 | 0.030 | 0.228 | 0.180 | Agerer (2001) |
| *V* | 0.008 | 0.037 | 0.205 | 0.176 | Wang *et al.* (2015) |
| *R* | 0.008 | 0.037 | 0.197 | 0.168 | Wang *et al.* (2015) |
| *I* | −0.003 | 0.033 | 0.198 | 0.162 | Wang *et al.* (2015) |
| *B* | 0.012 | 0.025 | 0.224 | 0.511 | This paper |
| *V* | 0.012 | 0.016 | 0.215 | 0.211 | This paper |
| $R_c$ | 0.009 | 0.015 | 0.213 | 0.207 | This paper |
| $I_c$ | 0.004 | 0.008 | 0.212 | 0.208 | This paper |

determined as follows: $a = 2.43R_{\odot}$, $R_1 = 1.34R_{\odot}$, $R_2 = 0.53R_{\odot}$, $L_1 = 6.29L_{\odot}$ and $L_2 = 0.71L_{\odot}$. Using the period–color relation determined by Wang (1994),

$$(B - V)_0 = 0.077 - 1.003 \log P \text{ (day)}. \tag{3}$$

We can calculate that the color index of V441 Lac is $(B - V)_0 = 0.59$. Then, by using the following equation taken from Rucinski & Duerbeck (1997),

$$M_v = -4.44 \log P + 3.02(B - V)_0 + 0.12. \tag{4}$$

We determined the absolute magnitude $M_V = 4.17$ mag. Based on Cox (2000), the $V$ band magnitude of V441 Lac can be estimated to be $m_V = 12.4$ mag. Accordingly, the distance modulus is calculated to be $m_V - M_V = 8.23$ mag, and the corresponding distance of about 442.6 pc can be derived.

Based on all available times of light minimum, we analyzed the orbital period variation of V441 Lac, and long term increase at a rate of $\mathrm{d}P/\mathrm{d}t = 5.874(\pm 0.007) \times 10^{-7}$ d yr$^{-1}$ was derived. This result is very similar with that determined by Wang *et al.* (2015). Using the well-known equation

$$\frac{\dot{P}}{P} = -3\dot{M}_1 \left( \frac{1}{M_1} - \frac{1}{M_2} \right), \tag{5}$$

the mass transfer from the secondary component to the primary can be calculated to be $\mathrm{d}M_1/\mathrm{d}t = 1.187(\pm 0.001) \times 10^{-7} M_{\odot}$ yr$^{-1}$. The positive sign reveals that the more massive primary component is the receiving mass. Table 6 shows some EW type binaries with low mass ratio ($q < 0.2$) and increasing orbital period. V441 Lac is very different from these systems. These systems have contact configurations, but V441 Lac is semi-detached. This makes V441 Lac a very interesting target.

In order to estimate the evolutionary state of V441 Lac, the two components of this system are displayed on the mass–luminosity diagram in Fig. 5, where the open circle represents the primary component, while the solid one refers to the secondary component. The solid and dotted lines show the Zero Age Main Sequence (ZAMS) and the Terminal Age Main Sequence (TAMS) lines constructed by the BSE Code (Hurley *et al.* 2002). As shown in Fig. 5, the more massive primary component is located below the ZAMS line, while the less massive secondary component is above

**Table 6.** Some EW type with low mass ratio ($q < 0.2$) and increasing orbital period.

| Stars | Period (days) | $q$ | Configuration | Increasing rate of the period (d yr$^{-1}$) | References |
|---|---|---|---|---|---|
| V410 Aur | 0.366340 | 0.143 | Contact | $8.2 \times 10^{-7}$ | Yang *et al.* (2005) |
| XY Boo | 0.370553 | 0.186 | Contact | $6.3 \times 10^{-7}$ | Yang *et al.* (2005) |
| V857 Her | 0.382229 | 0.065 | Contact | $2.9 \times 10^{-7}$ | Qian *et al.* (2005) |
| AH Cnc | 0.360441 | 0.168 | Contact | $4.0 \times 10^{-7}$ | Qian *et al.* (2006) |
| V1191 Cyg | 0.313377 | 0.107 | Contact | $4.5 \times 10^{-7}$ | Zhu *et al.* (2011) |
| V728 Her | 0.471289 | 0.160 | Contact | $1.9 \times 10^{-8}$ | Erkan & Ulaş (2016) |
| V441 Lac | 0.308915 | 0.093 | Semi-detached | $5.9 \times 10^{-7}$ | This paper |

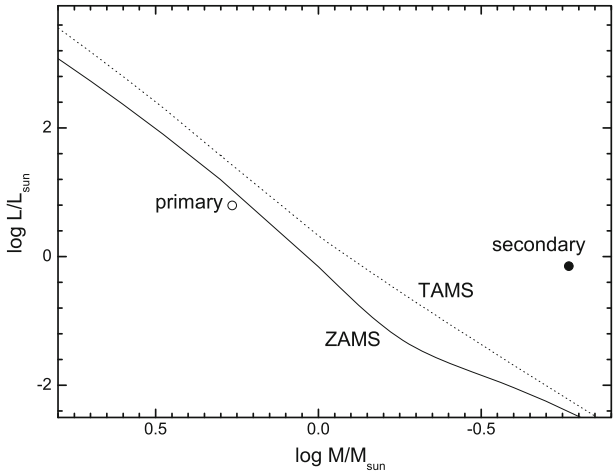


**Figure 5.** Mass–luminosity diagram of V441 Lac. The open circle represents the primary component, while the solid one shows the secondary component. The solid and dotted lines show the ZAMS and TAMS lines, constructed by the BSE code (Hurley *et al.* 2002).

the TAMS line, indicating that the primary is under-luminous and the secondary is over-luminous and over-sized. This is corresponding to Algol type eclipsing binaries.

V441 Lac is an EW type eclipsing binary. Normally, EW type eclipsing binaries are contact binaries. But our solutions show that V441 Lac is a semi-detached Algol type binary. The formation and evolution of such a system is worth studying. A possible formation process for this system is: this object is originally a W-subtype shallow contact binary, and the less massive secondary component is transferring mass to the more massive primary; with the mass transferring, this binary will evolve to the more shallow contact state and expand and finally the contact configuration destroys as predicted by the Thermal Relaxation Oscillation (TRO) models (e.g., Lucy 1976; Flannery 1976; Robertson & Eggleton 1977; Rahunen 1981). As predicted by the TRO theory, close binaries undergo oscillations around the state of marginal contact. Each oscillation contains a contact and a semi-detached phase. V441 Lac is undergoing the semi-detached phase. This system is a very good target to prove the TRO theory. In future, spectroscopic and photometric observations are needed to confirm the mass ratio and to determine the orbital evolution and the possibility of third components.

## Acknowledgements

This work is partly supported by the National Natural Science Foundation of China (No. U1431105) and by the Natural Science Foundation of Shandong Province (No. ZR2014AQ019), and by Young Scholars Program of Shandong University, Weihai, and by the Open Research Program of Key Laboratory for the Structure and Evolution of Celestial Objects (No. OP201303). The authors would like to thank the anonymous referee for very helpful suggestions and comments.

## References


Agerer, F. 2001, *IBVS*, **5024**, 1.
Agerer, F., Hubscher, J. 2002, *IBVS*, **5296**, 1.
Agerer, F., Hubscher, J. 2003, *IBVS*, **5484**, 1.
Cox, A. N. 2000, Allen's astrophysical quantities, 4th ed., AIP Press; Springer, New York.
Erkan, N., Ulaş, B. 2016, *NewA*, **46**, 73.
Flannery, B. P. 1976, *ApJ*, **205**, 217.
Hubscher, J. 2011, *IBVS*, 5984.
Hu, S. M., Han, S. H., Guo, D. F., Du, J. J. 2014, *RAA*, **14**, 719.
Hurley, J. R., Tout, C. A., Pols, O. R. 2002, *MNRAS*, **329**, 897.
Lee, Jae Woo, Hinse, Tobias Cornelius, Park, Jang-Ho 2013, *AJ*, **145**, 100.
Li, K., Qian, S.-B., Hu, S.-M., He, J.-J. 2014, *AJ*, **147**, 98.
Liao, W.-P., Qian, S.-B., Liu, N.-P. 2012, *AJ*, **144**, 178.
Lucy, L. B. 1976, *ApJ*, **205**, 208.
Morrison, J. E., Röser, S., McLean, B., Bucciarelli, B., Lasker, B. 2001, *AJ*, **121**, 1752.
Paschke, A., Brat, L. 2006, *OEJV*, **23**, 135.
Qian, S.-B., Zhu, L.-Y., Soonthornthum, B., Yuan, J.-Z., Yang, Y.-G., He, J.-J. 2005, *AJ*, **130**, 1206.
Qian, S.-B., Liu, L., Soonthornthum, B., Zhu, L.-Y., He, J.-J. 2006, *AJ*, **131**, 3028.
Qian, S.-B., Yuan, J.-Z., Soonthornthum, B., Zhu, L.-Y., He, J.-J., Yang, Y.-G. 2007, *ApJ*, **671**, 811.
Rahunen, T. 1981, *A&A*, **102**, 81.
Robertson, J. A., Eggleton, P. P. 1977, *MNRAS*, **179**, 359.
Rucinski, S. M., Duerbeck, H. W. 1997, *PASP*, **109**, 1340.
Samus, N. N., Goranskii, V. P., Durlevich, O. V. *et al.* 2003, *Astron. Lett.*, **29**, 468.
Terrell, D., Wilson, R. E. 2005, *Ap&SS*, **296**, 221.
Van Hamme, W. 1993, *AJ*, **106**, 2096.
von Zeipel, H. 1924, *MNRAS*, **84**, 665.
Wang, J.-M. 1994, *ApJ*, **434**, 277.
Wang, D., Zhang, L., Han, X. L., Agerer, F., Pi, Q., Wang, S. 2015, *NewA*, **36**, 32.
Wilson, R. E. 1990, *ApJ*, **356**, 613.
Wilson, R. E. 1994, *PASP*, **106**, 921.
Wilson, R. E., Devinney, E. J. 1971, *ApJ*, **166**, 605.
Yang, Y.-G., Qian, S.-B., Zhu, L.-Y. 2005, *AJ*, **130**, 2252.
Zacharias, N., Monet, D. G., Levine, S. E., Urban, S. E., Gaume, R., Wycoff, G. L. 2004, *AAS*, **205**, 4815.
Zhu, L. Y., Qian, S. B., Soonthornthum, B., He, J. J., Liu, L. 2011, *AJ*, **142**, 124.
Zhu, L. Y., Qian, S. B., Liu, N. P., Liu, L., Jiang, L. Q. 2013, *AJ*, **145**, 39.